RSC Advances

ROYAL SOCIETY OF CHEMISTRY

www.rsc.org/advances

Hofmeister anion effect on the formation of ZIF-8 with tuneable morphologies and textural properties from stoichiometric precursors in aqueous ammonia solution

Binling Chen,[a] Fenghua Bai,[a,b] Yanqiu Zhu[a] and Yongde Xia[a*]

[a] College of Engineering, Mathematics and Physical Sciences, University of Exeter, Exeter EX4 4QF, United Kingdom.

E-mail: y.xia@exeter.ac.uk; Tel: +44 1392 723683.

[b] School of Chemistry and Chemical Engineering, Inner Mongolia University, Hohhot 010021, Inner Mongolia, People's Republic of China

Abstract

In this report, a series of anions were demonstrated to remarkably affect and promote the formation of ZIF-8 from stoichiometric molar ratio of precursors in aqueous ammonia solution at room temperature. The requirement of ammonia concentration for the formation of pure ZIF-8 phase can be readily modulated by the anion. In addition, the anion types and concentrations can effectively promote the formation of pure ZIF-8 phase with tuneable particle morphologies and textural properties. The anion effect capacity was revealed to be $SO_4^{2-} > CH_3COO^- > Cl^- > Br^- > NO_3^-$, which follows the classic Hofmeister anion sequence.

1 Introduction

As a new sub-family of metal-organic frameworks, zeolitic imidazolate frameworks (ZIFs) consist of M-Im-M (where M is Zn, Co and Im stands for imidazolate linker) which is usually formed by a self-assembly approach. The diverse structures of ZIFs are similar to traditional aluminosilicate zeolites, where typically Zn^{2+} ions play the role of silicon while the imidazolate anions form bridges that mimic the role of oxygen in zeolite frameworks, with the M-Im-M angle around 145^{o}.[1] Consequently, ZIFs are novel porous materials with ultrahigh surface area and exhibit unique crystal structures mimicking aluminosilicate zeolites,[1, 2] which have attracted increasing attention for their promising and potential applications, such as gas separation and storage,[1-3] catalysis,[4-6] sensing[7-9] and drug delivery.[10, 11] A variety of approaches such as solvothermal method[5, 12-16] and hydrothermal method[17-19] for the synthesis of ZIFs have been extensively investigated, and the different parameters, such as solvents,[18, 20] temperatures[17, 21] and deprotonate agents,[13, 17, 20, 22, 23] that affect the ZIF formations, have also been widely discussed.[24] However, one particular parameter that may affect the ZIFs formation – the effect of anions, has not been explored yet. Considering that dramatic salt effects on the formation mechanisms and the morphologies of supramolecular materials have been observed,[25] it is of highly interest to understand whether anions may potentially have significant influence on the formation of ZIF materials.

The Hofmeister series of anions were initially developed in the research of protein solubility,[25] and the orders of anions with decreasing effect are as follows: SO_4^{2-}, HPO_4^{2-}, OH^-, F^-, $HCOO^-$, CH_3COO^-, Cl^-, Br^-, NO_3^-, I^-, SCN^-, ClO_4^-.[25] In the past, the effects of Hofmeister anions on the formation process of mesoporous silica have been examined and it was claimed that Hofmeister anions offer a wide range of possibilities to modulate the morphologies, stabilities and surface properties of mesoporous silicas.[25] For instance, Takashi and co-workers demonstrated that the effect of anion counteranion on the formation of

mesoporous materials under the acidic synthesis process,[26] while Zhao's group studied the anion sequence in the phase transformation of mesostructures.[27] Moreover, anion effect on the formation of metal based supramolecular complexes was also reported. It was found that the radius of anion played an important role in the formation of the structure and luminescent intensity of the Cd based coordination frameworks,[28] it is even claimed that Cd(II) coordination frameworks obtained from various anions can result in anion-induced structural transformation and anion-responsive photoluminescence.[29] In addition, reports of the anion effect on the formation of metal based supramolecular complexes , such as silver (I) complexes[30] and zinc (II) complexes,[31] can be also found in literature. These previous work encouraged us to explore the salt effect on the formation of ZIFs in this work.

Herein, for the first time, we reported our recent findings on the effect of anions on the formation of ZIF-8 materials. It is found that the introduction of anions (SO_4^{2-}, CH_3COO^-, Cl^-, Br^-, NO_3^-) into the reaction media of aqueous ammonia system, accelerates the self-assembly of stoichiometric zinc ions with the 2-methylimidazole (MIm) linker (1:2) and results in the formation of pure ZIF-8 with tuneable morphologies and textural properties. Our findings indicated that: 1) the requirement of aqueous ammonia concentrations for the formation of pure ZIF-8 is modulated by the anion types; 2) the generation of pure ZIF-8 materials is promoted by the anion concentrations and the anion types, which follows the rule of Hofmeister anion effect, as shown in Scheme 1.

2 Experimental

2.1 Materials

2-methylimidazole (99%, MIm), $Zn(NO_3)_2 \cdot 6H_2O$ (99%), $ZnSO_4$, $ZnCl_2$, $ZnBr_2$, $Zn(OAc)_2$, $NaNO_3$, Na_2SO_4, NaCl, NaBr, NaOAc, and 35 wt% ammonia aqueous solution were obtained from Sigma-Aldrich and used without further purification.

2.2 Materials synthesis

ZIF-8 was synthesized by rapid pouring an aqueous solution of zinc salts into an aqueous ammonia solution of 2-methylimidazole and the mixture was stirred at room temperature for 24 h. In a typical synthesis, zinc salt and corresponding sodium salt dissolved in distilled water was added into a solution of MIm in distilled water, where 35 wt% ammonia solution was added in the water beforehand. After aging for 24 hours at room temperature, the product was collected by repeated centrifugation (6000 rpm, 10 min). The resulting powders were then air dried in a fume cupboard for several days before subject to further characterizations.

2.3 Materials characterisation

X-ray diffraction (XRD) patterns were recorded with Cu Kα radiation (40 kV-40 mA) at step time 1 s and step size of 0.02^{o}. Fourier-transform infrared (FTIR) spectra were obtained in Alpha Bruker system. The samples were measured in the wavenumber range of 2000-500 cm^{-1}. Thermogravimetric analysis (TGA)/ differential thermal analysis (DTA) was performed on a TA SDT Q600 instrument from room temperature to 800 ^{o}C with a heating rate of 10 ^{o}C/min under a continuous air flow of 100 mL/min. A Hiden QGA gas analysis mass spectrometer (MS) was coupled with the Q600 instrument to monitor and detect the gaseous compositions in the exhaust emission. Scanning electron microscopy (SEM) images were recorded using a Philips XL-30 scanning electron microscope in a high vacuum mode and at an acceleration voltage of 20 kV. Samples were mounted using a conductive carbon double-sided sticky tape. A thin (*ca.* 10 nm) coating of gold was sputtered onto the samples to reduce the effects of charging. N_2 gas sorptions were carried out on a Quantachrome Autosorb-iQ gas sorptometer via conventional volumetric technique. Before gas analysis, the sample was evacuated for 4 h at 250 °C under vacuum. The textural properties were determined via nitrogen sorption at -196 °C. The surface area was calculated using the Brunauer-Emmett-

Teller (BET) method based on adsorption data in the partial pressure (*P*/*P*o) range of 0.02-0.22. The total pore volume was determined from the amount of nitrogen adsorbed at *P*/*P*o of ca. 0.99.

3 Results and discussion

3.1 Effect of ammonia concentrations on the formation of ZIF-8

The effect of ammonia concentrations on the formation of ZIF-8 was first investigated using different zinc salts in aqueous system, where stoichiometric molar ratio of 1:2 for Zn^{2+}/MIm was used. From the XRD patterns in Fig. 1, it is clear that lower ammonia concentrations result in the formation of impurity in the product, while higher ammonia concentrations can generate pure ZIF-8, which is in agreement with previous reports.[17, 32] Taking SO_4^{2-} as an example (Fig. 1a), the products derived from the molar ratios of Zn^{2+}/NH_3 < 1:75 are mixture of ZIF-8 and a dense *dia*(Zn) impurity,[21] but the products from molar ratios of $Zn^{2+}/NH_3 \geq$ 1:75 exhibit pure sodalite (SOD)-type structures in their XRD patterns. While other different anion zinc salts such as CH_3COO^-, Cl^-, Br^- or NO_3^- were used, the XRD patterns of the products (shown in Fig. 1 b-e) revealed that the molar ratios of $Zn^{2+}/NH_3 \geq$ 1:100, 1:200, 1:400 or 1:20 were required to form pure ZIF-8, with the yield of 75%, 70%, 67% and 85%, respectively. These results also indicate that the requirement of ammonia concentrations for the formation of pure ZIF-8 phase is modulated by the anion types. The morphologies of pure ZIF-8, which were obtained from different anion zinc salts at high ammonia concentrations, exclusively exhibited equilibrium rhombic dodecahedral particle shapes (Fig. 2).[33] In addition, the textural properties of the resulting ZIF-8 materials, as shown in Fig. 3, are clearly variable for samples from different anion zinc salts, implying that the anion types can dramatic affect the textural properties of the samples even if they are obtained under the same conditions.

3.2 Effect of additional anions on the formation of ZIF-8

In order to determine whether the introduction of additional anions can influence on the formation of ZIF-8 phase, a variety of anion sodium salts including Na_2SO_4, CH_3COONa (NaOAc), NaCl, NaBr, and $NaNO_3$ were separately added as additional anion sources, to the reaction media containing zinc salts with the same anion for one batch synthesis. Based on the results in Fig. 1, we chose the lowest ammonia concentration required for the formation of mixture of ZIF-8 and *dia*(Zn) phase to determine whether the presence of extra anions in the synthesis media can promote the transformation the formation of mixture to pure ZIF-8 phase. For example, the synthesis product from the molar ratio of $ZnSO_4$:MIm:NH_3=1:2:50 is a mixture. However, with the introducing of increased amount of Na_2SO_4 into the synthesis system, interestingly the impurity *dia*(Zn) in the product was gradually reduced and pure ZIF-8 was eventually formed with the molar ratio of $ZnSO_4$:Na_2SO_4 =1:15 (as shown in Fig. 4a), suggesting that the additional SO_4^{2-} indeed accelerates the formation of pure ZIF-8 phase. The Fourier-transform infrared (FTIR) spectrum for all the as-synthesised samples, including both ZIF-8 material and the impurity *dia*(Zn) containing composites (as shown in Fig. 4b), demonstrated similar spectra, probably due to the fact that the *dia*(Zn) has some similar functional groups with ZIF-8. Moreover, SEM images (Fig.4 c-e) clearly show that with the introduction of increased additional SO_4^{2-} into the reaction media, the morphologies of the products changed significantly from irregular rough-surface particle shapes to regular smooth-surface ZIF-8 with rhombic dodecahedral particle shapes.

Fig 5a shows the thermal gravimetric analysis (TGA) of the as-synthesised samples performed under air flow. Two weight loss events centred at 450 and 500 ^oC were observed, corresponding to the decomposition of organic species and the buring of the formed carbon species with the release of H_2O, CO_2 and NO_2 (see Fig 5c and d). In addition, two exothermic

peaks centred at 450 and 500 ^{o}C were demonstrated in DTA curves, which is consistent with the TGA results. Obviously, no SO_2 signal was detected (shown in Fig 5e) by MS, indicating no sulfate residuals existed in the as-synthesised samples. Interestingly, the TGA (Fig. 5a) result shows that residual weight precentage of the heated samples is decreased with the increasing of the amount of Na_2SO_4, suggesting that the promotive formation of crystalline ZIF-8 may lead to residual weight decreasing, as the impurity *dia*(Zn) is the quite dense *dia* framework reported by Qi et al.[21] The yield of the synthesised products is 95%, 91%, 85%, 77% and 76% with $ZnSO_4$:MIm:NH_3:Na_2SO_4 molar ratio of 1:2:50, 1:2:50:5, 1:2:50:10, 1:2:50:15, and 1:2:50:20, respectively. Obviously, the product yield decreases with the addtion amount of Na_2SO_4, due to the formation of highly porous ZIF-8 material under high Na_2SO_4 concentration, which is also consistent with TGA results.

In addition, as presented in Fig. 6, with the increase in the concentrations of SO_4^{2-} in the synthesis system, all the products exclusively exhibit type I nitrogen sorption isotherms with micropore domination; however, compared with the sample without additional Na_2SO_4, the sample from $ZnSO_4$:Na_2SO_4 = 1:20 exhibited up to 50% increase in both the specific surface area and total pore volume, remarkably changing from 1015 to 1576 m^2 g^{-1} and 0.49 to 0.74 cm^3 g^{-1} respectively. Obviously, the introduction of additional SO_4^{2-} anions effectively promotes the formation of pure ZIF-8 phase with variable particle morphologies and textural properties.

Other anion sodium salts such as NaOAc, NaCl and NaBr were also introduced into the synthesis system and it was found that the transformation from the mixture of ZIF-8 and dense *dia*(Zn) phase to pure ZIF-8 could be also readily realised when the molar ratio of zinc ion/sodium anion salt is higher than 1:20, 1:30 and 1:20 for NaOAc, NaCl and NaBr respectively (shown in Fig. 7a-c). However, the addition of $NaNO_3$ into the synthesis media of Zn^{2+}:MIm:NH_3 =1:2:15, which is the lowest ammonia concentration for the formation of a

mixture (as demonstrated in Fig. 1e), has not observable effect on the formation of pure ZIF-8 and the XRD patterns were kept unchanged even if the molar ratio of $Zn(NO_3)_2$:$NaNO_3$ is up to 1:30 (shown in Fig. 7d), indicating that NO_3^- has the weakest anion effect on the modulation of pure ZIF-8 generation among the studied anions. In addition, SEM images clearly show that the introduction of increased additional anions into the synthesis system results in the morphologies of the product were evolved remarkably from irregular rough-surface particles to regular smooth-surface ZIF-8 particles with rhombic dodecahedral shape (seen Fig. 8). Based on the results above, it is clear that except NO_3^-, the presence of anion sodium salts with appropriate anion concentrations in the synthesis solution can effectively accelerate the formation of pure ZIF-8 phase with adjustable particle morphologies.

3.3 Effect of anion capability on the formation of pure ZIF-8

To find out the anion effect capability on the formation of pure ZIF-8 phase, different anion sodium salts with various concentrations were introduced into a reaction solution with fixed molar ratio of Zn^{2+}:MIm:NH_3=1:2:50 (namely a synthesis system with the same ammonia concentration). It is surprising to note that except $NaNO_3$, pure ZIF-8 can be readily formed because of the presence of additional anion sodium salts, as shown in Fig. 9. Most strikingly, it can be summarised from the XRD results in Fig. 4a and Fig. 9 that the lowest molar ratio of Zn^{2+}:anion sodium salt, where the anions include SO_4^{2-}, CH_3COO^-, Cl^-, Br^- and NO_3^-, that leads to the formation of pure ZIF-8 phase is 1:15, 1:20, 1:40, 1:60 and nil, respectively. Combined the above observed NO_3^- has the weakest anion effect on the modulation of pure ZIF-8 formation, we can reasonable to conclude that the anion effect capacity on the formation of pure ZIF-8 phase from our experimental results is SO_4^{2-} > CH_3COO^- > Cl^- > Br^- > NO_3^-, which is in agreement with the classic Hofmeister anion sequence.[25]

Due to the fact that anions have negative charges, there could be interactions between zinc ions and the anions in the synthesis system. Anions could also interact with the protons that are deprotonated from the 2-methylimidazole ligand, and this interaction could be helpful for the protons to react easily with OH^- from ammonia solution, which is hypothesised to initiate the formation of ZIF-8.[17, 24] As various anions have different radii effect and dehydration effect in the aqueous system,[25-27] these effects lead to the different abilities to interact with zinc ions and protons, and also lead to the final observed orders which follows the classic Hofmeister anion sequence. Therefore, it is believed that additional anions can not only promote the formation of pure ZIF-8 phase, but also affect the properties of obtained ZIF-8 materials.

When considering the properties of Hofmeister anions in order, the charge is always the fundamental ionic property [25]. Therefore, due to the higher charge, SO_4^{2-} owns the strongest Hofmesiter effect. For the anions with the same charge, their size such as the Pauling radius plays an important role on comparing the capability of Hofmeister anion sequence. Based on the Pauling radius data,[34, 35] the order of the radii effect should be $Br^- > Cl^- > NO_3^- > CH_3COO^-$. In addition, the free energy or the entropy of hydration which measures the interaction of anions with water, is another fundamental property. The order of dehydration effect should be $SO_4^{2-} > CH_3COO^- > Cl^- > Br^- > NO_3^-$ anions.[34, 35] It should be noted that SO_4^{2-} presents a hydration free energy (-258.2 kcal/mol) which is about three times larger than that of other listed anions,[35] indicating that SO_4^{2-} has a strong interaction with the protons deprotonated from the 2-methylimidazole. As a result, the interplay of the radii effect and the dahydration effect gives rise to the observed anion sequence which follows the classic Hofmeister anion sequence.

4 Conclusions

In conclusion, a series of anions that affects the formation of ZIF-8 in aqueous ammonia systems has been demonstrated. The requirement of ammonia concentration for the generation of pure ZIF-8 phase can be modulated by the anions. In addition, the anion types and concentration remarkably influence on the formation of pure ZIF-8 and the anion effect capacity follows the classic Hofmeister anion sequence. The Hofmeister anion effect is important to better understand the formation mechanism of ZIFs in different systems and is also useful in other research areas such as interface chemistry.

Acknowldegement

The financial support by the Royal Society, the Royal Academy of Engineering and University of Exeter is greatly acknowledged.

References

1. A. Phan, C. J. Doonan, F. J. Uribe-Romo, C. B. Knobler, M. O'Keeffe and O. M. Yaghi, *Acc. Chem. Res.*, 2009, **43**, 58-67.
2. R. Banerjee, A. Phan, B. Wang, C. Knobler, H. Furukawa, M. O'Keeffe and O. M. Yaghi, *Science*, 2008, **319**, 939-943.
3. W. Zhou, H. Wu and T. Yildirim, *J. Am. Chem. Soc.*, 2008, **130**, 15268-15269.
4. K. Li, D. H. Olson, J. Seidel, T. J. Emge, H. Gong, H. Zeng and J. Li, *J. Am. Chem. Soc.*, 2009, **131**, 10368-10369.
5. H. Bux, F. Liang, Y. Li, J. Cravillon, M. Wiebcke and J. Caro, *J. Am. Chem. Soc.*, 2009, **131**, 16000-16001.
6. Y. Liu, E. Hu, E. A. Khan and Z. Lai, *J. Membr. Sci.*, 2010, **353**, 36-40.
7. H.-L. Jiang, B. Liu, T. Akita, M. Haruta, H. Sakurai and Q. Xu, *J. Am. Chem. Soc.*, 2009, **131**, 11302-11303.
8. C. Chizallet, S. Lazare, D. Bazer-Bachi, F. Bonnier, V. Lecocq, E. Soyer, A.-A. Quoineaud and N. Bats, *J. Am. Chem. Soc.*, 2010, **132**, 12365-12377.
9. U. P. N. Tran, K. K. A. Le and N. T. S. Phan, *ACS Catal.*, 2011, **1**, 120-127.
10. G. Lu and J. T. Hupp, *J. Am. Chem. Soc.*, 2010, **132**, 7832-7833.
11. S. Liu, Z. Xiang, Z. Hu, X. Zheng and D. Cao, *J. Mater. Chem.*, 2011, **21**, 6649-6653.
12. X.-C. Huang, Y.-Y. Lin, J.-P. Zhang and X.-M. Chen, *Angew. Chem. Int. Ed.*, 2006, **45**, 1557-1559.
13. Y.-Q. Tian, Y.-M. Zhao, Z.-X. Chen, G.-N. Zhang, L.-H. Weng and D.-Y. Zhao, *Chem. Eur. J.*, 2007, **13**, 4146-4154.
14. J. Cravillon, S. Münzer, S.-J. Lohmeier, A. Feldhoff, K. Huber and M. Wiebcke, *Chem. Mater.*, 2009, **21**, 1410-1412.

15. S. R. Venna, J. B. Jasinski and M. A. Carreon, *J. Am. Chem. Soc.*, 2010, **132**, 18030-18033.
16. K. S. Park, Z. Ni, A. P. Côté, J. Y. Choi, R. Huang, F. J. Uribe-Romo, H. K. Chae, M. O'Keeffe and O. M. Yaghi, *PNAS*, 2006, **103**, 10186-10191.
17. B. Chen, F. Bai, Y. Zhu and Y. Xia, *Microporous Mesoporous Mater.*, 2014, **193**, 7-14.
18. Y. Pan, Y. Liu, G. Zeng, L. Zhao and Z. Lai, *Chem. Commun.*, 2011, **47**, 2071-2073.
19. K. Kida, M. Okita, K. Fujita, S. Tanaka and Y. Miyake, *CrystEngComm*, 2013, **15**, 1794-1801.
20. J. Cravillon, R. Nayuk, S. Springer, A. Feldhoff, K. Huber and M. Wiebcke, *Chem. Mater.*, 2011, **23**, 2130-2141.
21. Q. Shi, Z. Chen, Z. Song, J. Li and J. Dong, *Angew. Chem. Int. Ed.*, 2011, **50**, 672-675.
22. W. Morris, C. J. Doonan, H. Furukawa, R. Banerjee and O. M. Yaghi, *J. Am. Chem. Soc.*, 2008, **130**, 12626-12627.
23. A. F. Gross, E. Sherman and J. J. Vajo, *Dalton Trans.*, 2012, **41**, 5458-5460.
24. B. Chen, Z. Yang, Y. Zhu and Y. Xia, *J. Mater. Chem. A*, 2014, *in press*, DOI: 10.1039/C4TA02984D.
25. E. Leontidis, *Curr. Opin. Colloid Interface Sci*, 2002, **7**, 81-91.
26. S. Che, S. Lim, M. Kaneda, H. Yoshitake, O. Terasaki and T. Tatsumi, *J. Am. Chem. Soc.*, 2002, **124**, 13962-13963.
27. J. Tang, C. Yu, X. Zhou, X. Yan and D. Zhao, *Chem. Commun. (Camb)*, 2004, 2240-2241.
28. Y.-T. Wang, S.-C. Yan, G.-M. Tang, C. Zhao, T.-D. Li and Y.-Z. Cui, *Inorg. Chim. Acta*, 2011, **376**, 492-499.
29. S. Hou, Q. K. Liu, J. P. Ma and Y. B. Dong, *Inorg. Chem.*, 2013, **52**, 3225-3235.

30. C.-W. Yeh, W.-J. Chang, M.-C. Suen, H.-T. Lee, H.-A. Tsai and C.-H. Tsou, *Polyhedron*, 2013, **61**, 151-160.

31. Y. Wen, T. Sheng, S. Hu, Y. Wang, C. Tan, X. Ma, Z. Xue, Y. Wang and X. Wu, *CrystEngComm*, 2013, **15**, 2714.

32. M. He, J. Yao, Q. Liu, K. Wang, F. Chen and H. Wang, *Microporous Mesoporous Mater.*, 2014, **184**, 55-60.

33. P. Y. Moh, M. Brenda, M. W. Anderson and M. P. Attfield, *CrystEngComm*, 2013, **15**, 9672-9678.

34. C. S. Babu and C. Lim, *J. Phys. Chem. B*, 1999, **103**, 7958-7968.

35. Y. Marcus, *J. Chem. Soc., Faraday Trans.*, 1991, **87**, 2995-2999.

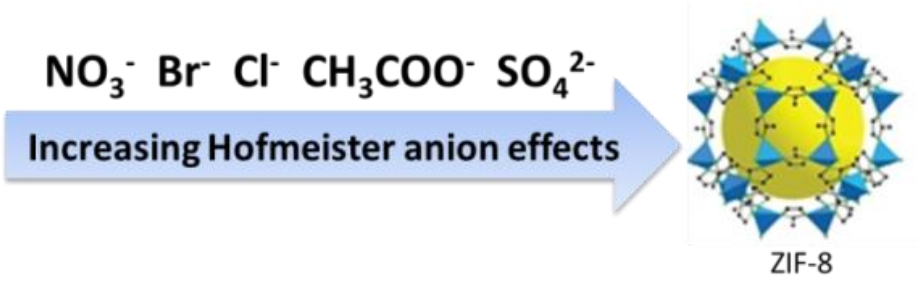

Scheme.1 Hofmeister anion effect on the formation of ZIF-8.

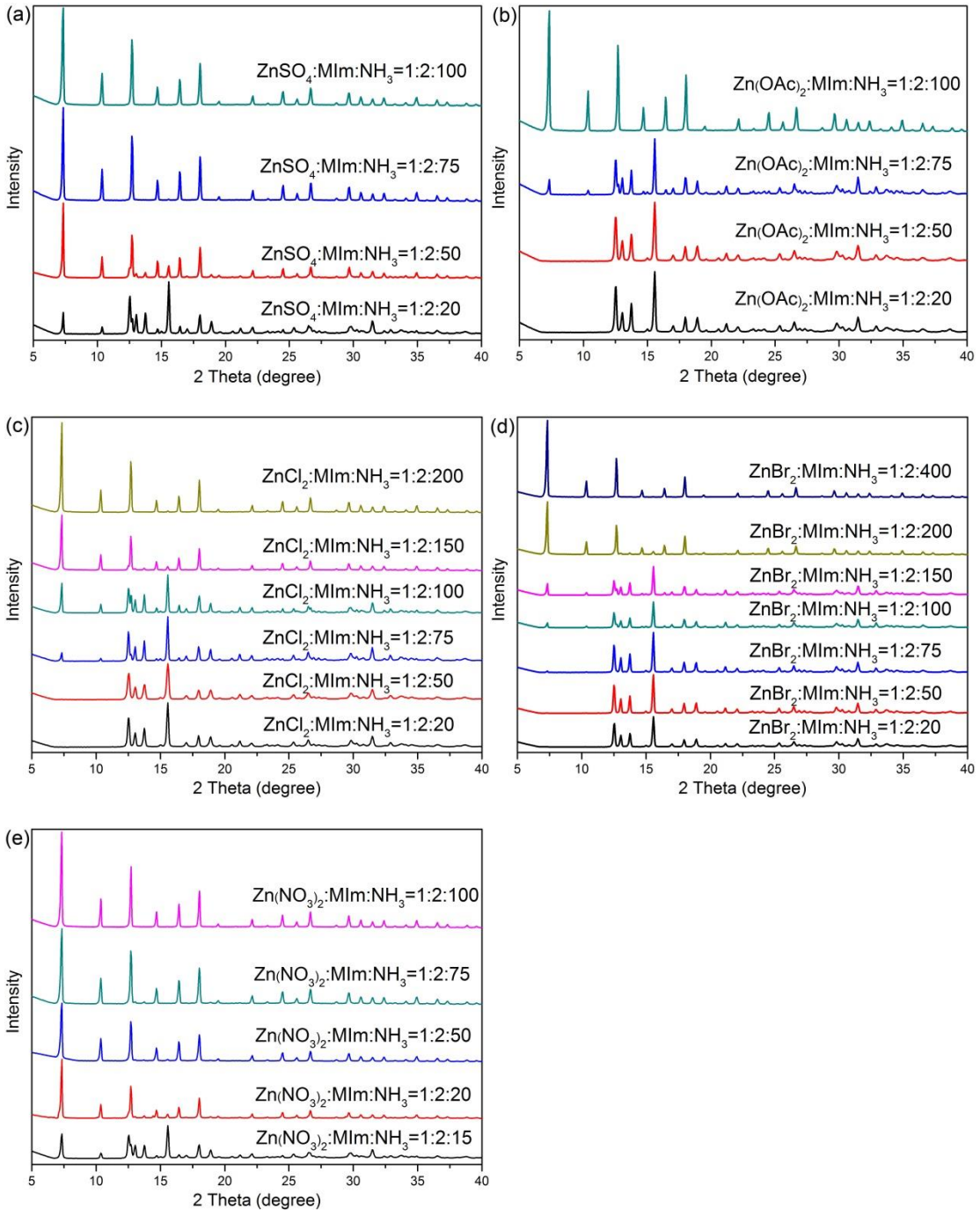

Fig. 1 XRD patterns of the as-synthesised samples in different concentrations of ammonia solution for variable zinc salts: (a) $ZnSO_4$ (b) $Zn(OAc)_2$, (c) $ZnCl_2$, (d) $ZnBr_2$, and (e) $Zn(NO_3)_2$, representatively.

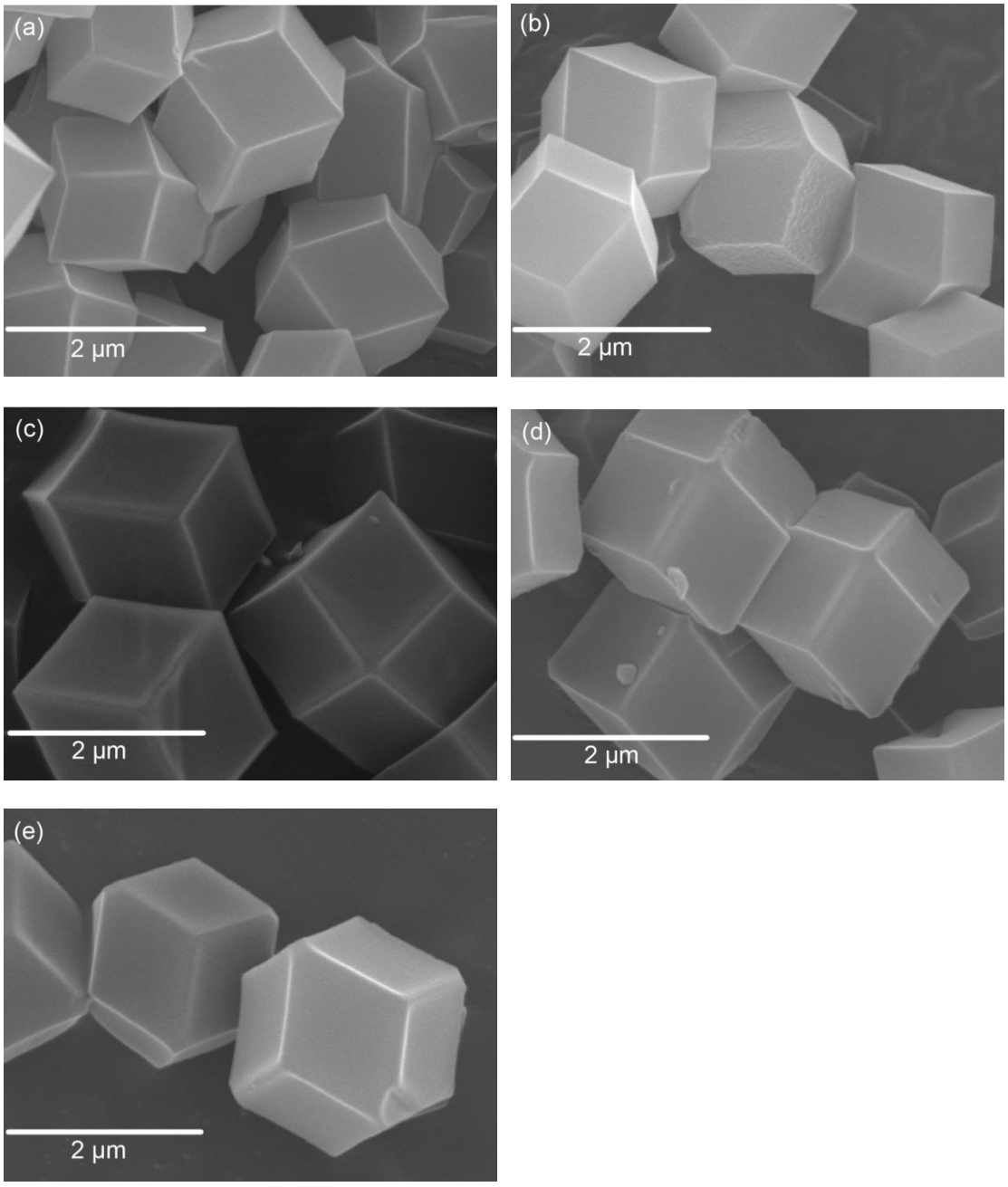

Fig. 2 Representative SEM images of as-synthesised ZIF-8 in ammonia solution with various anions: (a) $ZnSO_4$:MIm:NH_3 =1:2:100; (b) $Zn(OAc)_2$:MIm:NH_3 = 1:2:100; (c) $ZnCl_2$:MIm:NH_3 =1:2:200; (d) $ZnBr_2$:MIm:NH_3 =1:2:400 and (e) $Zn(NO_3)_2$:MIm:NH_3 =1:2:100, respectively.

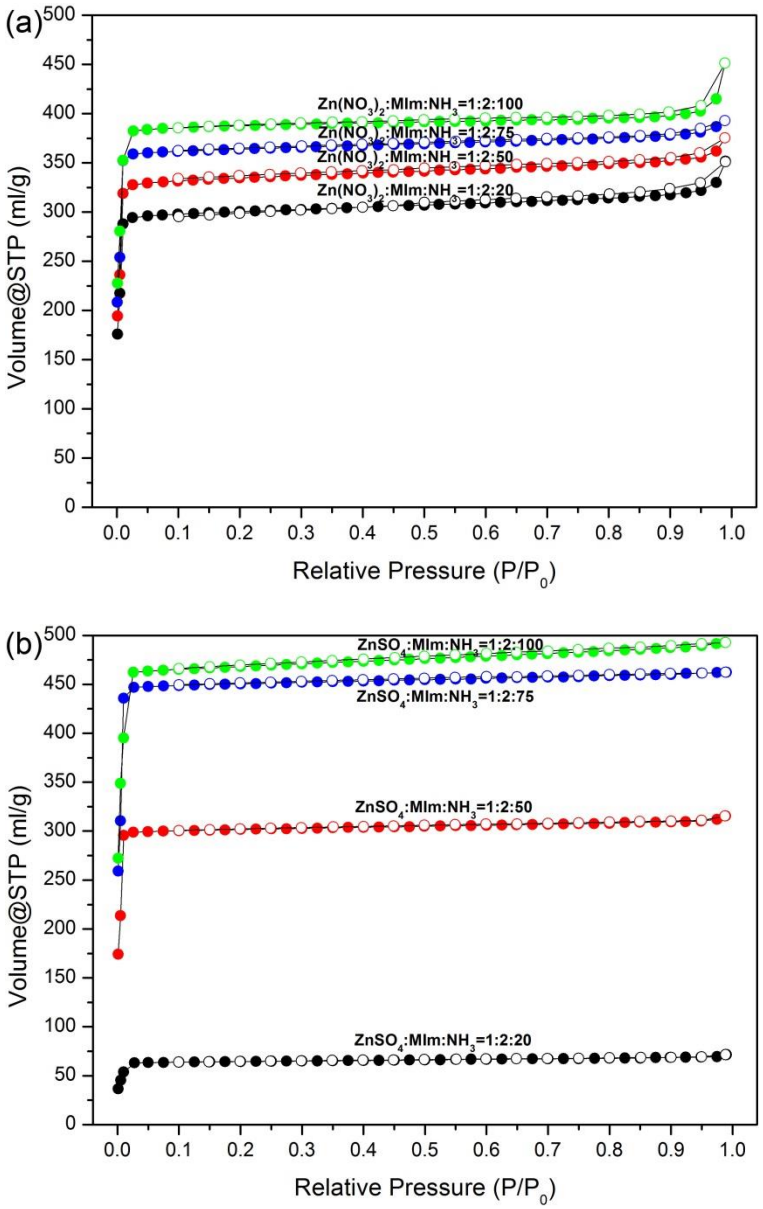

Fig. 3 Nitrogen sorption isotherms of as-synthesised ZIF-8 derived from different anion zinc salt in various concentrations of aqueous ammonia solution. (a) $Zn(NO_3)_2$ and (b) $ZnSO_4$. Solid and hollow data correspond to the adsorption and desorption branches, respectively.

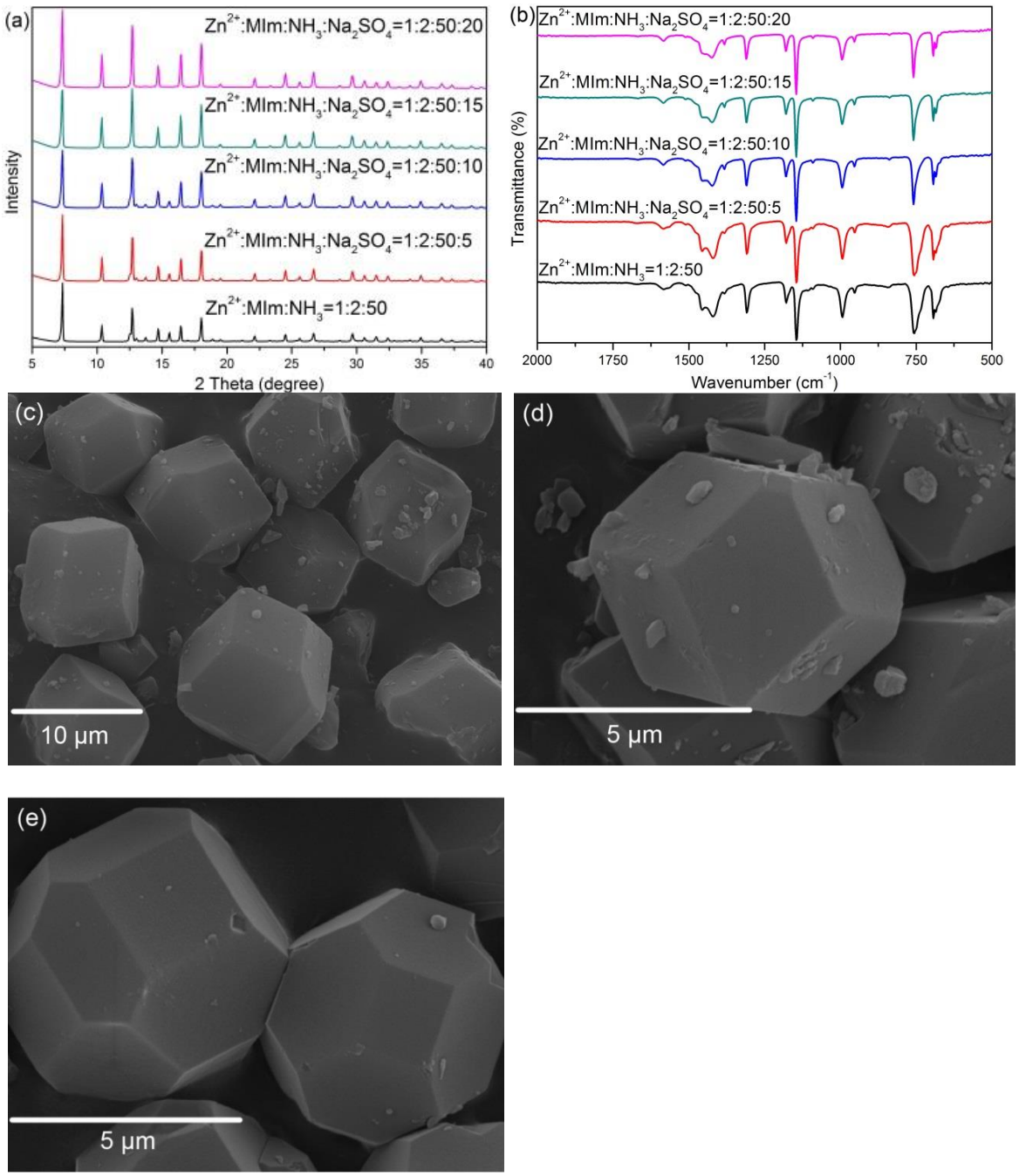

Fig. 4 (a) XRD patterns and (b) FTIR spectrum of the as-synthesised samples in different concentrations of sodium sulfate; (c-e) SEM images of as-synthesised samples in ammonia solution with Zn^{2+}:MIm:NH_3: Na_2SO_4 molar ratios of 1:2:50, 1:2:50:5 and 1:2:50:20, respectively.

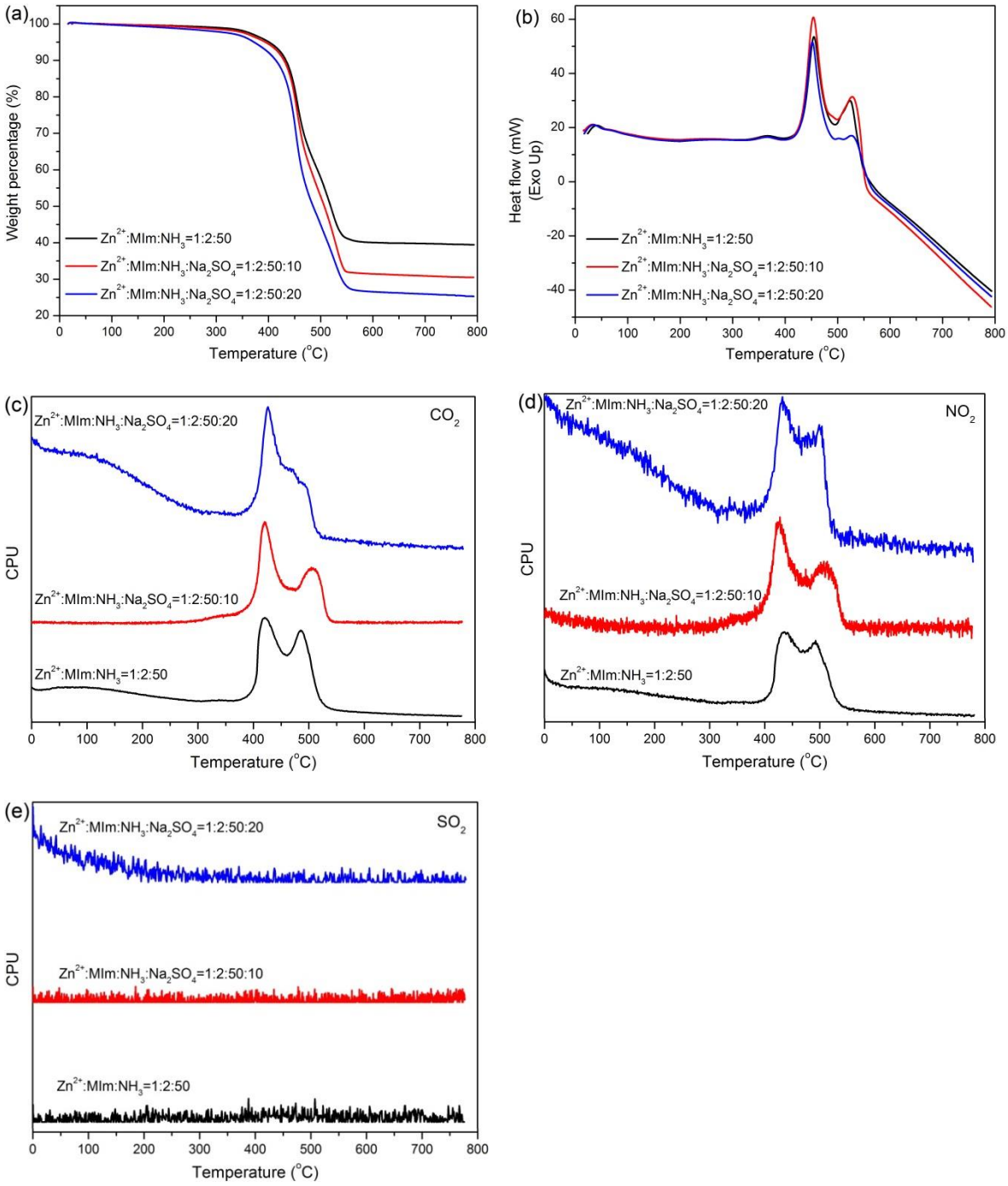

Fig. 5 (a) TGA curves, (b) corresponding DTA curves and (c-e) MS signals for different as-synthesised samples heated in air atmosphere.

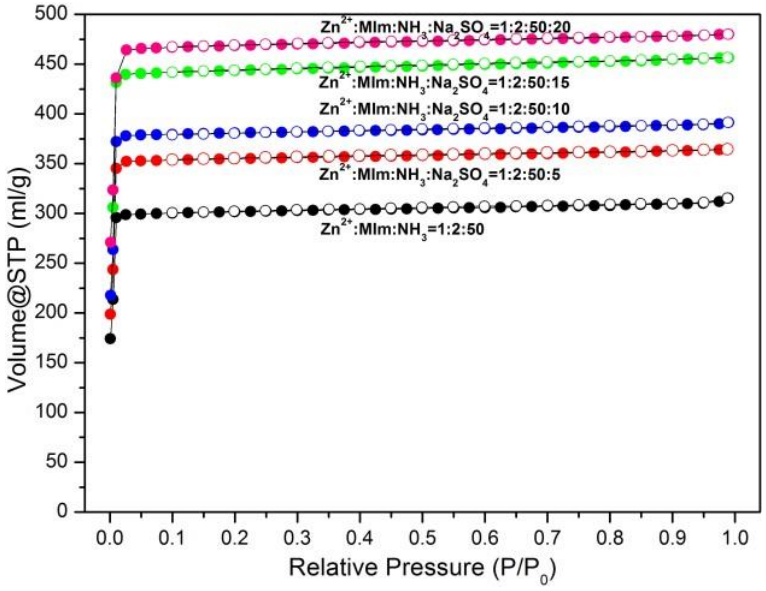

Fig. 6 Nitrogen sorption isotherms of as-synthesised ZIF-8 under different concentrations of sodium sulfate. The solid and hollow cycle correspond to the adsorption and desorption branches, respectively.

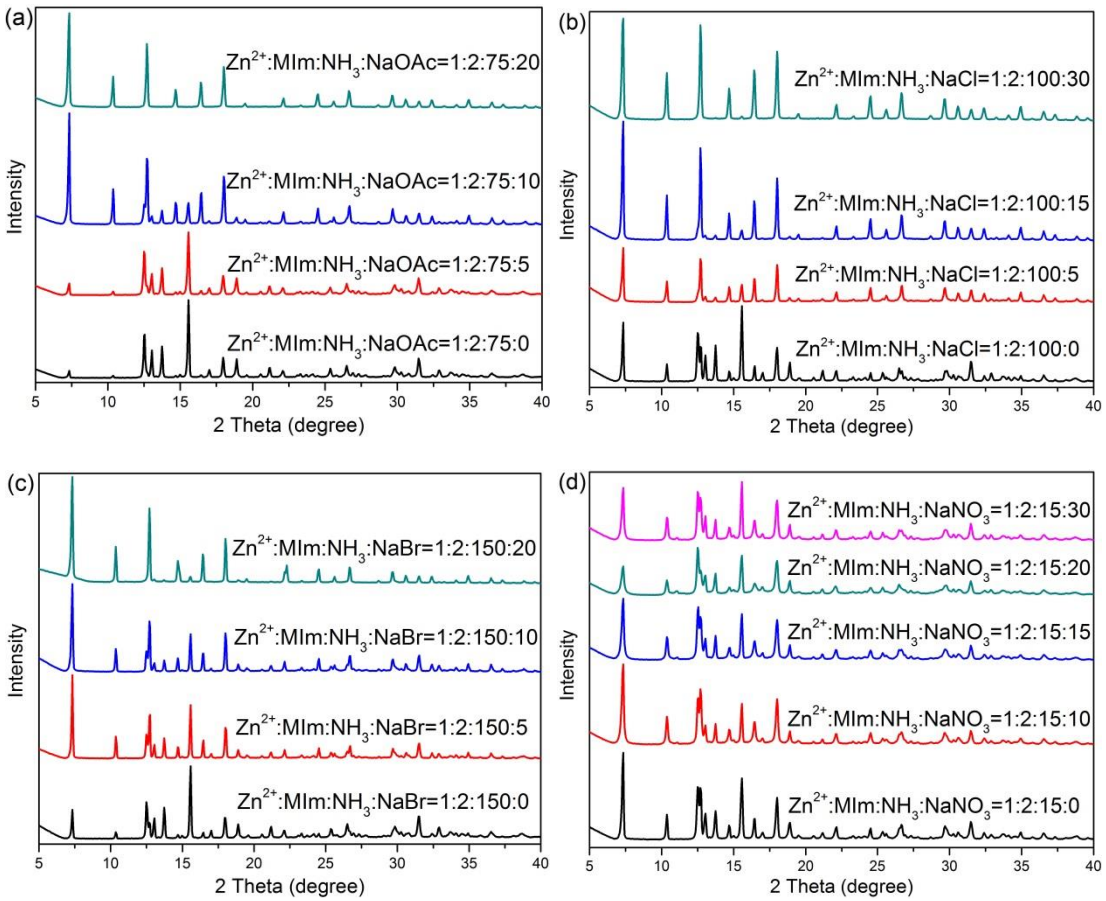

Fig. 7 XRD patterns of the as-synthesised samples in different concentrations of ammonia solution for variable zinc salts with the additional anions: (a) NaOAc, (b) NaCl, (c) NaBr, and (d)$NaNO_3$, representatively.

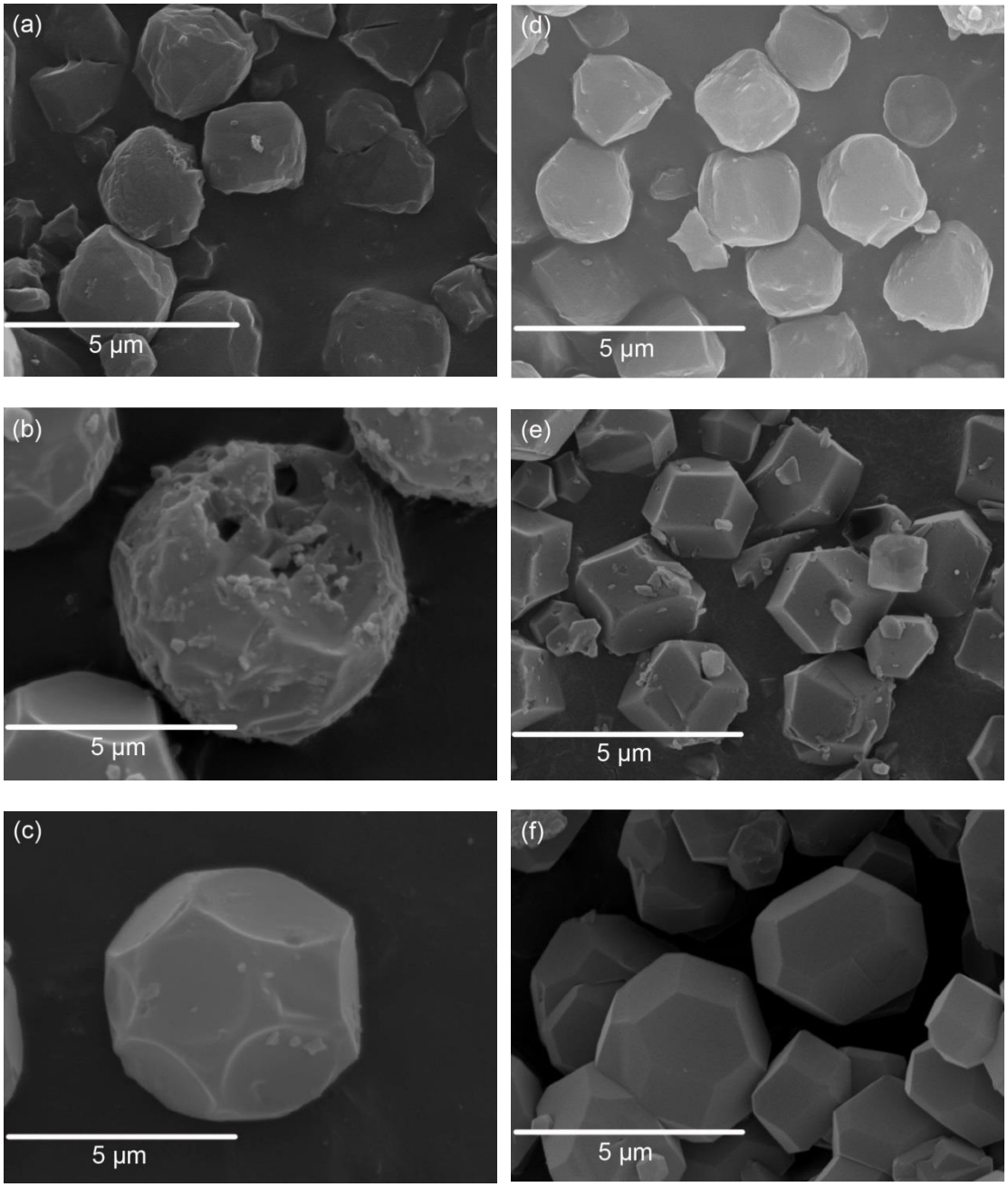

Fig. 8 Representative SEM images of as-synthesised products in ammonia solution from different anion sodium salts (a, b and c) NaOAc and (d, c and e) NaCl with various additional anion concentrations: (a) Zn^{2+} : MIm : NH_3 = 1 : 2 : 75; (b) Zn^{2+} : MIm : NH_3 : NaOAc = 1 : 2 : 75 : 10; (c) Zn^{2+} : MIm : NH_3 : NaOAc = 1 : 2 : 75 : 20; (d) Zn^{2+} : MIm : NH_3 = 1 : 2 : 100; (e) Zn^{2+} : MIm : NH_3 : NaCl = 1 : 2 : 100 : 5; (f) Zn^{2+} : MIm : NH_3 : NaCl = 1 : 2 : 100 : 30, respectively.

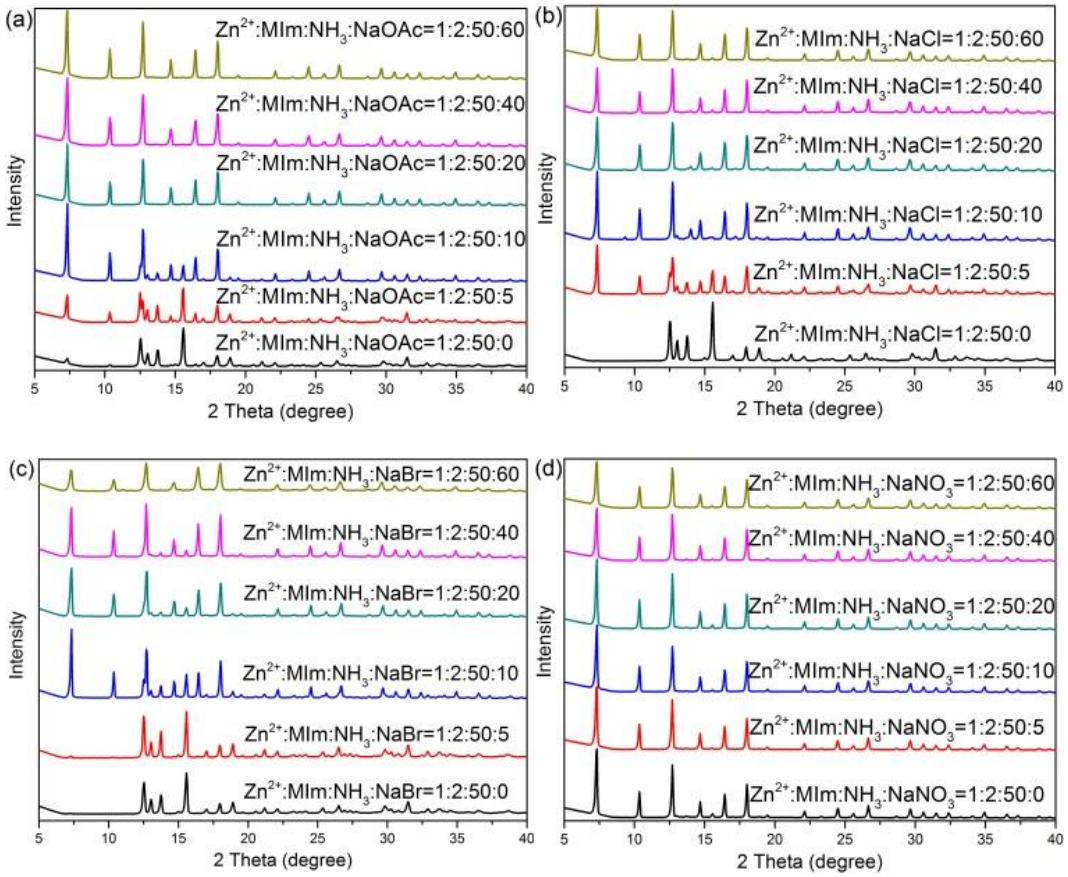

Fig. 9 XRD patterns of the samples derived from a same concentration of aqueous ammonia solution with the introduction of additional of (a) NaOAc, (b) NaCl, (c) NaBr and (d) $NaNO_3$, respectively.

Table of Content:

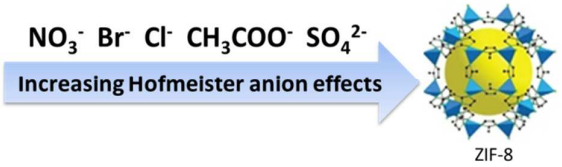

The classic Hofmeister anions can remarkably affect and promote the formation of ZIF-8 with tuneable particle morphologies and textural properties.